

Features of Inelastic and Elastic Characteristics of Si and SiO₂/Si Structures

A.P. Onanko¹, V.V. Kuryliuk¹, Y.A. Onanko², A.M. Kuryliuk¹, D.V. Charnyi², O.P. Dmytrenko¹,
M.P. Kulish¹, T.M. Pinchuk-Rugal¹

¹ Taras Shevchenko National University of Kyiv, 64/13, Volodymyrska St., 01601 Kyiv, Ukraine

² Institute of Water Problems and Land Reclamation, 37, Vasyliivska St., 03022 Kyiv, Ukraine

(Received 11 August 2021; revised manuscript received 20 October 2021; published online 25 October 2021)

Measurement of temperature dependences of internal friction (IF) was performed on identical Si *p*-type substrates, orientation (100), doped with boron B, with specific resistivity $\rho \approx 7.5 \text{ Ohm}\cdot\text{cm}$ and thickness $h \approx 4.7 \cdot 10^5 \text{ nm}$. The samples passed the same technological route after deposition of a SiO₂ layer with thickness $h \approx 600 \text{ nm}$ because of high-temperature oxidation in dry O₂ at $T_0 \approx 1300 \text{ K}$. It was found that the annealing of structural defects in Si changes the shape of the IF temperature spectrum $Q^{-1}(T)$. The IF peaks Q_M^{-1} formed by point defects could be observed under the condition that Si was heated at a rate $V = \Delta T / \Delta t \leq 0.1 \text{ K/s}$. After X-ray irradiation with a dose $\gamma \approx 104 \text{ R}$, the IF maximum at $T_{M1} \approx 320 \text{ K}$ increases sharply; its height Q^{-1}_{M1} increases almost threefold with a twofold decrease in the width ΔQ^{-1}_{M1} , which testifies to the process of relaxation of radiation defects of the same type. The activation energy value $H_1 \approx 0.63 \text{ eV}$ was obtained for the IF peak Q_M^{-1} in the Si plate at $T_{M1} \approx 320 \text{ K}$. The proximity of the obtained activation energy H_1 at $T_{M1} \approx 320 \text{ K}$ to the migration energy $H_0 \approx 0.85 \text{ eV}$ for positively charged interstitial atoms Si⁺ suggests a relaxation mechanism due to the reorientation of interstitial atoms Si⁺. Upon electron irradiation, as a result of the collision of electrons with Si atoms, Frenkel defects are formed. Calculations show that the electron energy $W \approx 1 \text{ MeV}$, which corresponds to the experiment, is sufficient to shift Si atoms from their equilibrium positions. After irradiation with a dose $\gamma \approx 105 \text{ R}$, the IF Q^{-1}_{M1} maximum height at $T_{M1} \approx 320 \text{ K}$ did not change significantly in comparison with the IF $Q^{-1}(T)$ spectrum before irradiation that indicates a special effect of the dose $\gamma \approx 105 \text{ R}$.

Keywords: Internal friction, Structural defects, Ultrasonic, Microstructure.

DOI: [10.21272/jnep.13\(5\).05017](https://doi.org/10.21272/jnep.13(5).05017)

PACS numbers: 82.33.Ln, 82.70.Gg, 83.80.Kn

1. INTRODUCTION

It is known that upon annealing of solid-state mixtures, the release of vacancies *V* from the material is observed. Defect annealing leads to a change in the shape of the internal friction (IF) temperature spectrum $Q^{-1}(T)$ [1-3]. The non-destructive IF method allows to set the spectrum of structural defects by analyzing the positions of the IF maxima, the duration of the relaxation time τ , and their deposition during damping of elastic vibrations. The criterion of structural relaxation does not determine the magnitude of the relaxation effect. Total deformation consists of elastic and inelastic constituents $\varepsilon_{\Sigma} = \varepsilon_E + \varepsilon_{AE}$ [4-6]. Elastic deformation ε_E occurs "instantly". Inelastic deformation ε_{AE} is conditioned by the motion of dislocations [5-7].

A method to control structural defects by measuring IF and elastic modulus *E* after laser radiation was developed. Studies of the influence of structural defects on damping of vibrations in Si/SiO₂ plates with diameter $D = 100 \pm 60 \text{ mm}$ and thicknesses $h_{\text{SiO}_2} \approx 600 \text{ nm}$ and $h_{\text{Si}} \approx 400000 \text{ nm}$ allow estimating the degree of perfection of the crystal structure. Measurement of the amplitude dependence of IF allows to establish the moment of separation of dislocation segments from stoppers.

The effects of acoustic emission (AE) under laser thermal-mechanical strains in SiO₂/TiO₂/ZrO₂ films are investigated.

2. MATERIALS AND METHODS

The IF inelastic Q^{-1} and elastic *E* characteristics significantly depend on the morphology of the surface layer. A 3D atomic-force microscopy (AFM) image of the SiO₂ microstructure on the Si(100) surface is represented in Fig. 1.



Fig. 1 – 3D AFM image of the SiO₂ microstructure on Si (100) ($1 \times 1 \times 10^3 \text{ nm}$)

The SiO₂ surface after laser irradiation is shown in Fig. 2. This process in a set of time phases mimics the "volcanic eruption".

The AE technique at $f_{\parallel} = 0.2 \div 0.5 \text{ MHz}$, $\alpha = 70 \text{ dB}$ was used to measure elastic wave velocities V_{\parallel} and V_{\perp} . The amplification of the recording equipment based on a specialized acoustic emission device AF-15 was $\alpha = 60 \text{ dB}$. The pulse power of the ruby laser was $I \approx 300 \text{ MW/cm}^2$, the pulse duration of the ruby laser was $\tau \approx 20 \text{ ns}$ with a wavelength $\lambda = 694 \text{ nm}$, and the

area of the laser spot was $S_0 \approx 1 \times 1 \text{ mm}^2$. Fig. 3 shows the AE pattern after irradiation of SiO_2 with the ruby laser.

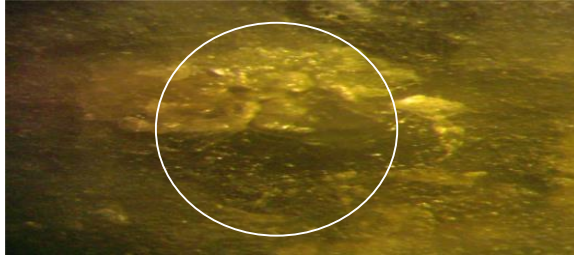


Fig. 2 – SiO_2 surface after nanosecond laser irradiation with the ruby laser with intensity $I \approx 300 \text{ MW/cm}^2$, dose $D = 4 \times I$, ruby laser pulse duration $\tau \approx 20 \text{ ns}$, wavelength $\lambda = 694 \text{ nm}$. The circle indicates the area of laser irradiation ($\times 56$)

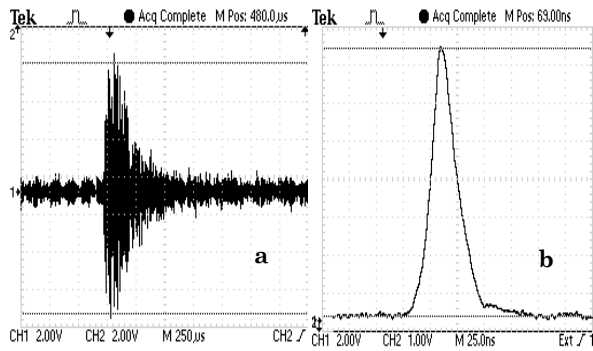


Fig. 3 – (a) AE after nanosecond laser irradiation of SiO_2 with the ruby laser with $I \approx 300 \text{ MW/cm}^2$, 2 V/p , $250 \mu\text{s/p}$; (b) ruby laser pulse width $\tau \approx 20 \text{ ns}$, wavelength $\lambda = 694 \text{ nm}$

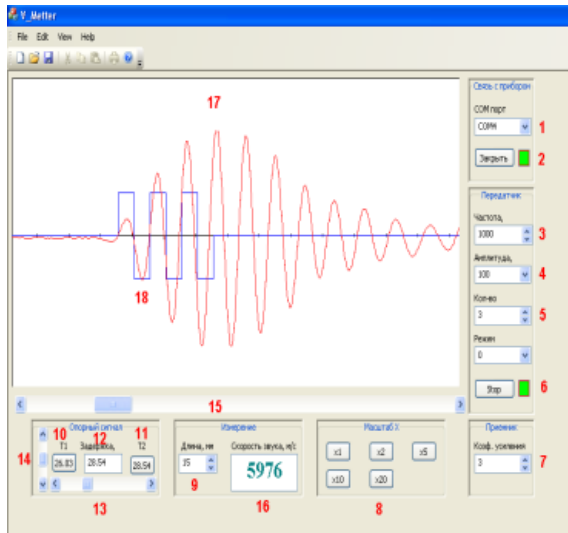


Fig. 4 – Illustration of the window for processing the data of measurements of the elastic wave velocity V_{\parallel} in the SiO_2/Si plate by the echo-pulse method at frequency $f_{\parallel} \approx 1 \text{ MHz}$ and in the presence of computer device KERN-4

Metallographic optical observations of the microstructure by means of a microscope LOMO MVT, AFM were used. Ultrasonic (US) pulse-phase method using USMV-LETI, modernized USMV-KNU and computerized “KERN-4” (Fig. 4 and Fig. 5) with frequencies $f_{\parallel} \approx 1 \text{ MHz}$ and $f_{\perp} \approx 0.7 \text{ MHz}$, US invariant-polarization method to determine effective

acoustic μ_{il} and elastic C_{ijkl} constants were used [8, 9]. The measured velocity error was $\Delta V/V = 0.5 \pm 1.5 \%$.

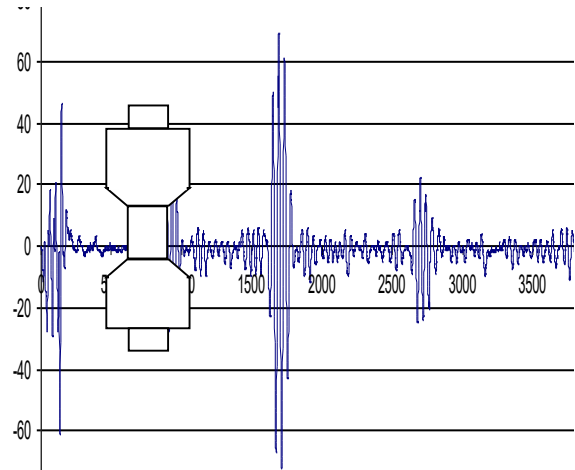


Fig. 5 – Disturbance source and receiver – piezo quartz (US sensor), sound in Si

The deformation behavior of the Si crystal was investigated using a Large-scale Atomic/Molecular Massively Parallel Simulator (LAMMPS). The Tersoff empirical potential was used to account for the interactions among silicon atoms. This version of the potential turned out to be reliable for studying strained silicon [10]. In the present simulation, silicon structures are initially annealed at a temperature of $T = 300 \text{ K}$ using a Nosé-Hoover thermostat for $5 \cdot 10^5$ time steps, where each step is separated by an interval of 1 fs . The velocity-Verlet algorithm is employed to integrate the equations of motion. After equilibration, the tensile simulations are performed using an NVT-ensemble at a constant rate $d\varepsilon/dt = 10^8 \text{ s}^{-1}$, typical of molecular dynamics (MD) simulations. Strain was created by continuously increasing the length of the simulation cell along the z -direction and remapping the coordinates of all atoms to a new cell after every 1 fs of MD simulation. To obtain the global stress σ_{ij} of the whole Si structure during deformation, the average stress per atom was computed from the virial theorem as follows:

$$\sigma_{ij} = \frac{1}{V} \left(\frac{1}{2} \sum_{\alpha=1}^N \sum_{\beta \neq \alpha}^N U(r^{\alpha\beta}) \frac{\Delta x_i^{\alpha\beta} \Delta x_j^{\alpha\beta}}{r^{\alpha\beta}} \right), \quad (1)$$

where N is the total number of atoms, $r^{\alpha\beta}$ is the distance between two atoms α and β , $\Delta x^{\alpha\beta} = x^\alpha - x^\beta$, U is the potential energy, and V is the volume of the structure.

Fig. 6 shows the stress-strain $\sigma(\varepsilon)$ curve of bulk Si subjected to uniaxial tensile loading at a temperature of 300 K , obtained with the Tersoff model. The model structure starts with a linear relation between stress σ and strain ε values in accordance with Hooke's law $\sigma = E \cdot \varepsilon$, where E is the elastic modulus. After the elastic region, the stress-strain curve becomes non-linear as the strain increases. The stress continues to rise to a peak point followed by a sudden drop, which is caused by the brittle fracture of silicon.

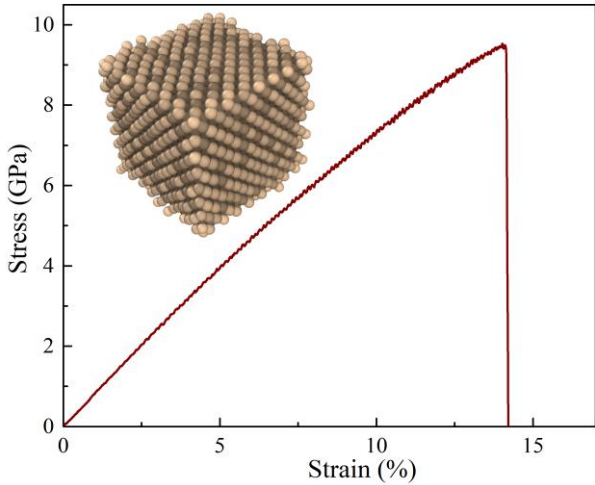


Fig. 6 – Stress-strain curve of single-crystalline Si obtained by MD simulation with Tersoff potential. On the inset: a simulated silicon cell

We then performed the estimation of the elastic modulus E from the slope of the stress-strain $\sigma(\varepsilon)$ curve presented in Fig. 6 in the elastic deformation range ($\varepsilon < 0.5\%$). The elastic modulus E of single-crystalline Si was 81 GPa, which is in agreement with the experimental data.

3. RESULTS AND DISCUSSION

An illustration of the measurement data on the "fast" quasi-transverse elastic wave velocity $V_{\perp 1[001]} = 3200 \pm 10$ m/s in Si by the echo pulse-phase technique at a frequency of $f_{\perp} = 0.7$ MHz is shown in Fig. 7. The obtained shear modulus is equal to $G_{001} = \rho V_{\perp 1[001]}^2 = 23.86$ GPa. The logarithmic decrement of US attenuation is

$$\delta = \ln\left(\frac{A_{n+1}}{A_n}\right) = \ln\left(\frac{73}{63}\right) \approx (1.47 \pm 0.1) \times 10^{-1}.$$

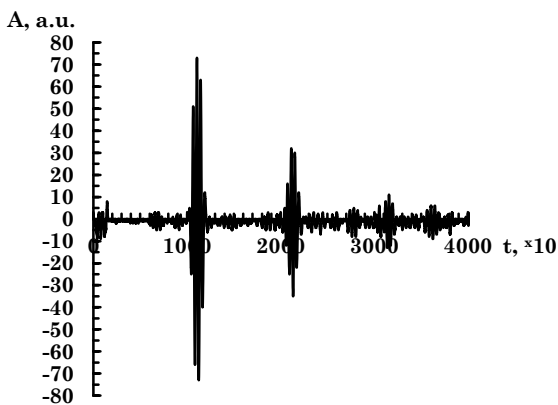


Fig. 7 – Pulse waveform with quasi-transverse "fast" polarization $V_{\perp 1}$ in the Si (100) plane. Logarithmic decrement of US attenuation $\delta = \ln\left(\frac{A_{n+1}}{A_n}\right) = \ln\left(\frac{73}{63}\right) \approx (1.47 \pm 0.1) \times 10^{-1}$

The quasi-longitudinal US velocity $V_{\parallel[001]} = 5870$ m/s and the elastic modulus $E_{001} = \rho V_{\parallel[001]}^2 = 80.28$ GPa were determined for SiO₂/Si from the oscillogram. The

temperature dependence of IF $Q^{-1}(T)$ (Fig. 8) and the elastic modulus $E(T)$ (Fig. 9) (indicatory surface of the inelastic-elastic body) of SiO₂/Si is shown in Fig. 10.

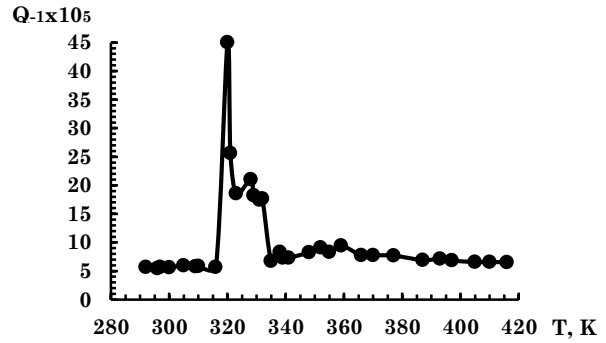


Fig. 8 – Temperature dependence of IF $Q^{-1}(T)^{-1}$ for SiO₂/Si plate

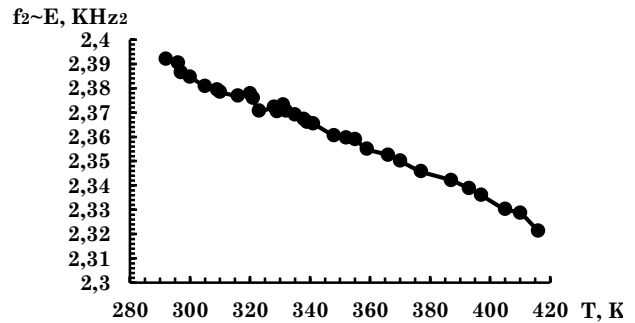


Fig. 9 – Temperature dependence of the square of the resonance frequency $f^2 \sim E$ for SiO₂/Si plate

The dependence of the height of the IF maximum on the radiation dose also indicates a relaxation process of reorientation of complexes of radiation defects. A small background value of IF $Q_0^{-1} \approx 2 \cdot 10^{-6}$ at $T \approx 385$ K is observed in the temperature dependence of IF $Q^{-1}(T)$ and the elastic modulus $E(T)$ (indicatory surface of the inelastic-elastic body) of SiO₂ after mechanical treatment in the initial state and annealing at $T_{an} \approx 670$ K for $t_{an} \approx 2100$ s in Fig. 10.

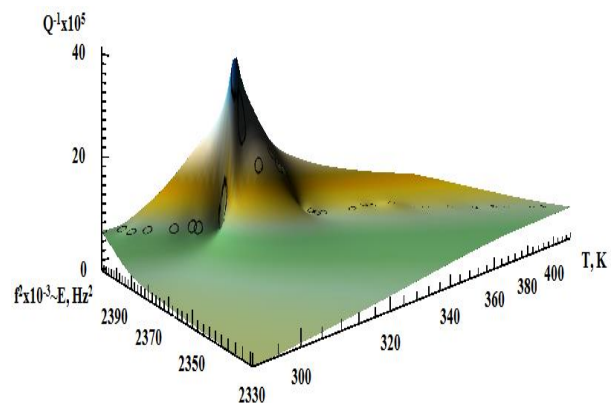


Fig. 10 – Temperature dependence of IF $Q^{-1}(T)$ and the elastic modulus $E(T)$ (indicatory surface of inelastic-elastic body) for SiO₂/Si plate

IF $Q^{-1} = \frac{\ln(\frac{A_1}{A_2})}{\pi}$, IF defect $\frac{\Delta Q^{-1}}{Q^{-1}} = \frac{Q_{sat}^{-1} - Q_{sk}^{-1}}{Q_{sk}^{-1}}$ in Fig. 11 and the US attenuation coefficient $\alpha = \frac{Q^{-1}}{\lambda} = \frac{Q^{-1}}{\frac{v}{f}} = \frac{\ln(\frac{A_0}{A_1})}{h}$ were determined from the oscillogram of pulses with the corresponding polarization $V_{\parallel[001]}$ in "dry" SiO₂ skeleton in Fig. 7 before and after saturation $V_{\parallel[001]}^S$ from the logarithm of amplitude ratios $A_1, A_2, (A_0 - \text{no sample})$.

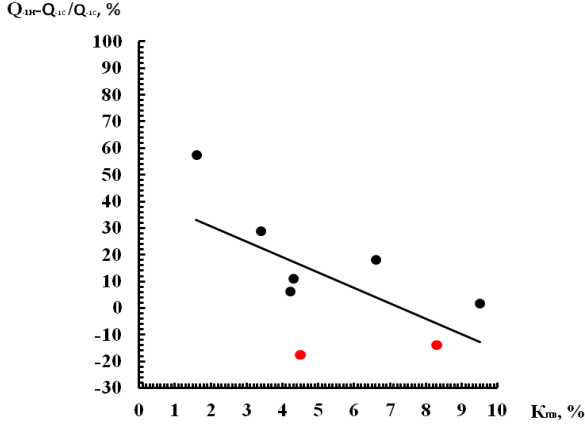


Fig. 11 – Correlation dependence of the IF defect $\Delta Q^{-1}/Q^{-1}$ in SiO₂ on the open porosity coefficient $K_{po} = V_{po}/V$

The complex elastic modulus of Si E^* is equal to the sum of the dynamic elastic modulus $E' = \rho V_{\parallel}^2$ and the loss modulus $E'' = E' \delta$ [5]:

$$E^* = E'(1 + \delta) = \rho V_{\parallel}^2(1 + \delta) = \rho V_{\parallel}^2(1 + \pi Q^{-1}), \quad (2)$$

where δ is the logarithmic decrement of the US attenuation, ρ is the Si specimen density, V_{\parallel} is the quasi-longitudinal US elastic wave velocity, and IF is equal to $Q^{-1} = \delta/\pi$.

$$\frac{E''}{E'} = \delta = \pi Q^{-1} = \alpha \lambda = \alpha \frac{v}{f}, \quad (3)$$

where α is the US attenuation coefficient, λ is the US wavelength, f is the US frequency. The logarithmic decrement of US attenuation δ of oscillations with amplitude $A = A_0 e^{-\delta x}$ is equal to

$$\delta = \ln\left(\frac{A_{n+1}}{A_n}\right). \quad (4)$$

The shear modulus $G = \rho V_{\perp}^2$, the dynamic elastic modulus E [5]:

$$E = \rho V_{\perp}^2 \left[3 + \frac{1}{1 - \left(\frac{V_{\parallel}}{V_{\perp}}\right)^2} \right], \quad (5)$$

where V_{\perp} is the quasi-transverse US velocity.

The Poisson coefficient μ is determined by the ratio of the relative transverse compression ε_{\perp} to the relative longitudinal elongation ε_{\parallel} and is equal to [6]:

$$\mu = -\frac{\varepsilon_{\perp}}{\varepsilon_{\parallel}} = -\frac{\frac{\Delta X}{X}}{\frac{\Delta l}{l}} = -\frac{\Delta X}{\Delta l} * \frac{l}{X}, \quad (6)$$

$$\mu = \frac{\frac{1}{2}V_{\parallel}^2 - V_{\perp}^2}{V_{\parallel}^2 - V_{\perp}^2}. \quad (7)$$

One oscillator produces 3 waves: 1 longitudinal and 2 transverse. Debye temperature θ_D is determined by the formula [7]:

$$\theta_D = \frac{h}{k_B} * \left(\frac{9N_A \rho}{4\pi A}\right)^{\frac{1}{3}} * \left(\frac{1}{V_{\parallel}^3} + \frac{2}{V_{\perp}^3}\right)^{\frac{1}{3}}, \quad (8)$$

where k_B is the Boltzmann constant, h is the Plank constant, N_A is the Avogadro number, A is the average gram-molecular weight.

For SiO₂, the Poisson coefficient $\mu = 0.2996$ and Debye temperature $\theta_D = 267.0$ K. For Si, the Poisson coefficient $\mu = 0.2097$ and Debye temperature $\theta_D = 309.3$ K.

The longitudinal wave velocity in liquid SiO₂ with an aqueous solution of NaCl with a concentration of $\rho \approx 38.125$ g/l was $V_{\parallel} \approx 2830$ m/s, the shear wave velocity was $V_{\perp} \approx 2300$ m/s, the Poisson coefficient was $\mu = 0.3032$ measured by AE technique.

4. CONCLUSIONS

1. The elastic modulus E , the shear modulus G , the Poisson coefficient μ and IF Q^{-1} depend on the anisotropy of SiO₂/Si plate.
2. The value of IF background Q_0^{-1} after thermal and mechanical treatments describes the changes in the elastic stress σ_i fields in SiO₂/Si plate.
3. It is found that, as a result of annealing of structural defects, IF background Q_0^{-1} significantly decreases when measuring the temperature dependence of IF $Q^{-1}(T)$, which indicates an improvement in the crystal structure of SiO₂/Si.
4. The study of vibrations of Si/SiO₂ disk plate at different harmonic frequencies f_0, f_2 made it possible to develop a technique for determining the density of structural defects n_D for semiconductor wafers-substrates.
5. The relationship between IF Q^{-1} , the logarithmic decrement of US attenuation δ and the dislocation density n_D is established for disk-shaped semiconductor wafers-substrates.
6. An increase in the IF maximum height Q_M^{-1} indicates an increase in the concentration of structural defects, and the broadening of the IF maximum ΔQ_M^{-1} here is a process of relaxation of new types of structural defects in SiO₂/Si plate.
7. The crater fusion depth Δh at a constant intensity I and laser irradiation time t is limited by local thermal conductivity and the establishment of "time-equilibrium" distribution of temperature gradients ΔT perpendicular to the crater axis and along it.
8. Outcomes of the evaluation of the dynamic characteristics of interstitial atoms S_i , vacancies V and O-complexes can be used to account the condition of annealing with the purpose of revealing specific structural defects in SiO₂/Si after laser radiation.

ACKNOWLEDGEMENTS

This work has been supported by the Ministry of Education and Science of Ukraine: Grant of the Ministry of Education and Science of Ukraine for the

prospective development of the scientific direction "Mathematical sciences and natural sciences" at Taras Shevchenko National University of Kyiv.

REFERENCES

1. A. Puskar, *Internal friction of materials* (Cambridge: Cambridge International Science Publishing: 2001).
2. M.S. Blanter, I.S. Golovin, H. Neuhauser, .-R. Sinning, A *handbook on internal friction in metallic materials* (Berlin: Springer Heidelberg: 2007).
3. R. Schaller, D. Mari, *Internal friction and mechanical spectroscopy* (Switzerland: Trans Tech Publication: 2012).
4. I.S. Golovin, Anelasticity, *internal friction and mechanical spectroscopy of metallic materials* (Moscow: Publishing company MISIS: 2020).
5. A.P. Onanko, *J. Metalphys. New Technol.* **33** No 2, 253 (2011).
6. A.P. Shpak, Y.A. Kunickiy, V.L. Karbovskiy, *Cluster and nano structural materials* (Kyiv: Academy periodicals: 2001).
7. I.S. Golovin, *Internal friction and mechanical spectroscopy of metal materials* (Moscow: Publishing company MISIS: 2012).
8. A.P. Onanko, V.V. Kuryliuk, Y.A. Onanko, A.M. Kuryliuk, D.V. Charnyi, M.P. Kulish, O.P. Dmytrenko, *J. Nano-Electron. Phys.*, **12** No 4, 04026 (2020).
9. Y.A. Onanko, A.P. Onanko, N.P. Kulish, *J. Metalphys. New Technol.* **33** No 13, 529 (2011).
10. V. Kuryliuk, O. Nepochatyi, P. Chantrenne, D.Lacroix, M. Isaiev, *J. Appl. Phys.* **126**, 055109 (2019).

Особливості непружних та пружних характеристик Si та SiO₂/Si структур

А.П. Онанко¹, В.В. Курилюк¹, Ю.А. Онанко², А.М. Курилюк¹, Д.В. Чарний², О.П. Дмитренко¹, М.П. Куліш¹, Т.М. Пінчук-Ругаль¹

¹ Київський національний університет імені Тараса Шевченка, вул. Володимирська, 64/13, 01601 Київ, Україна

² Інститут водних проблем і меліорації, вул. Васильківська, 37, 03022 Київ, Україна

Вимірювання температурних залежностей внутрішнього тертя (ВТ) проводилося на ідентичних, що пройшли один і той же технологічний маршрут, підкладках Si *p*-типу, орієнтації (100), легованого бором В, з питомим електроопором $\rho \approx 7,5$ Ом·см, товщиною $h \approx 4.7 \cdot 10^5$ нм після нанесення на них шару SiO₂ товщиною $h \approx 600$ нм в результаті високотемпературного окислення в сухому O₂ при $T_0 \approx 1300$ К. В процесі вимірювань було встановлено, що відпал структурних дефектів Si змінює форму температурного спектру ВТ. Піки ВТ Q^{-1}_M , що утворюються точковими дефектами, можна було спостерігати при умові, коли підкладка Si нагрівалася зі швидкістю $V = \Delta T / \Delta t \leq 0.1$ К/с. Після рентгенівського опромінення дозою $\gamma \approx 10^4$ Р максимум ВТ при $T_M \approx 320$ К різко зростає; його висота Q^{-1}_{M1} збільшується майже у 3 рази при зменшенні вдвічі ширини ΔQ^{-1}_{M1} , що свідчить про проходження процесу релаксації одного типу радіаційних дефектів. Для піка ВТ в підкладці Si при $T_M \approx 320$ К було отримано значення енергії активації $H_1 \approx 0,63$ еВ. Близькість отриманого нами значення енергії активації H_1 при $T_M \approx 320$ К до енергії міграції для додатно заряджених міжвузлових атомів Si⁺ $H_0 \approx 0,85$ еВ дозволяє припустити релаксаційний механізм, що обумовлений переорієнтацією міжвузлових атомів Si. При електронному опроміненні в результаті зіткнення електронів з атомами Si відбувається утворення дефектів по Френкелю. Оцінки показують, що енергія електронів $W \approx 1$ МеВ, яка відповідає експерименту, достатня для зміщення атомів Si із своїх рівноважних положень. Після опромінення дозою $\gamma \approx 10^5$ Р висота максимуму Q^{-1}_{M1} при $T_M \approx 320$ К в порівнянні зі спектром ВТ до опромінення істотно не змінилася, що свідчить про особливий вплив дози $\gamma \approx 10^5$ Р.

Ключові слова: Внутрішнє тертя, Структурні дефекти, Ультразвуковий, Мікроструктура.